

$X(3872)$ and $Y(4140)$ using diquark-antidiquark operators with lattice QCD

M. Padmanath* and C. B. Lang†

Institute of Physics, University of Graz, A-8010 Graz, Austria

S. Prelovsek‡

*Department of Physics, University of Ljubljana, Jadranska 19, 1000 Ljubljana, Slovenia**Jozef Stefan Institute, Jadranska 19, 1000 Ljubljana, Slovenia and**Theory Center, Jefferson Lab, 12000 Jefferson Avenue, Newport News, Virginia 23606, USA*

We perform a lattice study of charmonium-like mesons with $J^{PC} = 1^{++}$ and three quark contents $\bar{c}d\bar{u}$, $\bar{c}c(\bar{u}u + \bar{d}d)$ and $\bar{c}c\bar{s}s$, where the later two can mix with $\bar{c}c$. This simulation with $N_f=2$ and $m_\pi \simeq 266$ MeV aims at the possible signatures of four-quark exotic states. We utilize a large basis of $\bar{c}c$, two-meson and diquark-antidiquark interpolating fields, with diquarks in both antitriplet and sextet color representations. A lattice candidate for $X(3872)$ with $I=0$ is observed very close to the experimental state only if both $\bar{c}c$ and $D\bar{D}^*$ interpolators are included; the candidate is not found if diquark-antidiquark and $D\bar{D}^*$ are used in the absence of $\bar{c}c$. No candidate for neutral or charged $X(3872)$, or any other exotic candidates are found in the $I=1$ channel. We also do not find signatures of exotic $\bar{c}c\bar{s}s$ candidates below 4.2 GeV, such as $Y(4140)$. Possible physics and methodology related reasons for that are discussed. Along the way, we present the diquark-antidiquark operators as linear combinations of the two-meson operators via the Fierz transformations.

I. INTRODUCTION

The experimental discovery of charged resonances $Z_c(3900)^+$ [1] and $Z(4430)^\pm$ [2, 3] gives signatures for hadrons with minimal quark content $\bar{c}c\bar{d}u$. The neutral $X(3872)$ and yet-unconfirmed $Y(4140)$ with charge parity $C = +1$ also appear to have significant four-quark Fock components. Most of the observed exotic states have $J^P = 1^+$. The J^P for some has not been settled experimentally and $J^P = 1^+$ presents one possible option.

In this paper, we perform a lattice investigation of the charmonium spectrum, looking for charmonium-like states with quantum numbers $J^{PC} = 1^{++}$ and three quark contents: $\bar{c}c\bar{d}u$, $\bar{c}c(\bar{u}u + \bar{d}d)$ and $\bar{c}c\bar{s}s$, where the later two channels have $I=0$ and can mix with $\bar{c}c$ (C indicates C -parity of neutral isospin partners for charged states). Our main interest in these channels is aimed at a first-principle study of $X(3872)$ and $Y(4140)$, which were observed in $X(3872) \rightarrow J/\psi\rho$, $J/\psi\omega$, $D\bar{D}^*$ and $Y(4140) \rightarrow J/\psi\phi$, for example.

From the experimental side, the long known exotic candidate $X(3872)$ [4] is confirmed to have $J^{PC} = 1^{++}$ [5]. However, questions about its isospin remain unsettled. If it has isospin $I=1$, one expects charged partners. Observation of a nearly equal branching fraction for $X(3872) \rightarrow J/\psi\omega$ and $X(3872) \rightarrow J/\psi\rho$ decays [6] and searches for charged partner $X(3872)$ states decaying to $J/\psi\rho^\pm$ [7] speak against a pure $I=1$ state. There are a few other candidates with $C=+1$ that could possibly have $J^{PC} = 1^{++}$ like $X(3940)$ [8], $Z(4050)^\pm$ [3] and $Z(4250)^\pm$ [3]. A detailed review on these can be found in Ref. [9].

The growing evidence for the $Y(4140)$ resonance in the $J/\psi\phi$ invariant mass [10] serves as promising signature for exotic hadrons with hidden strangeness. Similarities in the properties of $X(3930)$ and $Y(4140)$ led to an interpretation that $X(3930)$ may be a $D^*\bar{D}^*$ molecule and $Y(4140)$ is its hidden strange counterpart $D_s^*D_s^*$ molecule [11]. However, the upper limit for the production of $Y(4140)$ in $\gamma\gamma \rightarrow J/\psi\phi$ is observed to be much lower than theoretical expectations for a $D_s^*D_s^*$ molecule with $J^{PC} = 0^{++}$ and 2^{++} [12]. Hence the quantum numbers of $Y(4140)$ stay unsettled and it remains open for a $J^{PC} = 1^{++}$ assignment.

From a theoretical perspective, the description of such resonances is not settled. Several suggestions have been made interpreting them as mesonic molecules [13], as diquark-antidiquark structures [14], as a cusp phenomena [15] or as a $|c\bar{c}g\rangle$ hybrid meson [16]. A great deal of theoretical studies are based on phenomenological approaches like quark model, (unitarized) effective field theory and QCD sum rules (see reviews [9]).

It is paramount to establish whether QCD supports the existence of resonances with exotic character using first principles techniques such as lattice QCD. Simulations that considered only $\bar{c}c$ interpolators could not provide evidence for $X(3872)$. The first evidence from a lattice simulation for $X(3872)$ with $I=0$ was reported in Ref. [17], where a combination of $\bar{c}c$ as well as $D\bar{D}^*$ and $J/\psi\omega$ interpolators was used. Recently, another calculation using the Highly Improved Staggered Quark action also gave evidence for $X(3872)$, using $\bar{c}c$ and $D\bar{D}^*$ interpolating fields [18]. The search for the $Y(4140)$ resonance was performed only in [19], where a phase shift for $J/\psi\phi$ scattering in s -wave and p -wave was extracted from $N_f=2+1$ simulation using twisted boundary conditions, and neglecting strange-quark annihilation. The resulting phase shifts did not support existence of a resonance.

The novel feature of the present study is to add

* padmanath.madanagopalan@uni-graz.at

† christian.lang@uni-graz.at

‡ sasa.prelovsek@ijs.si

diquark-antidiquark $[\bar{c}\bar{q}]_{\mathcal{G}}[cq]_{\mathcal{G}}$ operators to the basis of interpolating fields and to extend the extraction of the charmonium spectrum with $J^{PC} = 1^{++}$ to a higher energy range. This is the first dynamical lattice calculation involving diquark-antidiquark operators along with several two-meson and $\bar{c}c$ kind of interpolators to study $X(3872)$ and $Y(4140)$. We consider the color structures $\mathcal{G} = \bar{3}_c, 6_c$ for diquarks, which have been suggested already in the late seventies [20]. Recently many phenomenological studies [14, 21] and a few lattice studies [22, 23] used them to extract the light and heavy meson spectra. In Ref. [23] a calculation using two-meson and diquark-antidiquark interpolators was performed to investigate mass spectrum of 1^{++} exotic mesons in quenched lattice QCD. However, only one energy level was extracted, which is not sufficient to provide evidence for $X(3872)$ or $Y(4140)$.

In this paper we address the following questions: Is the lattice candidate for $X(3872)$ reproduced in presence of diquark-antidiquark operators? Which are the crucial operator structures for its emergence? How important are the $[\bar{c}\bar{q}]_{\mathcal{G}}[cq]_{\mathcal{G}}$ Fock components in the established $X(3872)$? Do we find a lattice candidate for charged or neutral $X(3872)$ with $I = 1$? Do operators with hidden strangeness render a candidate for $Y(4140)$? Do we find candidate states for other possible exotic states in the channels being probed?

The paper is organized as follows. Section II addresses the expected two-meson scattering channels below 4.2 GeV. The lattice methodology is discussed in Sect. III. In Sect. IV and the Appendix we discuss the relations between our diquark-antidiquark and two-meson interpolators via Fierz transformations. Section V is dedicated to results and we conclude in Sect. VI.

II. TWO PARTICLE STATES IN LATTICE QCD

A major hurdle in excited-state spectroscopy is that most of the states lie above various thresholds and decay strongly in experiments. All states carrying the same quantum numbers, including the single-particle and multiparticle states, in principle contribute to the eigenstates of the Hamiltonian. The determination of scattering properties relies on precise identification of all the eigenstates below and close above the energy of our interest. The continuous spectrum of scattering states in the continuum gets reduced to a discrete set of eigenstates, because lattice momenta are discretized due to the finite lattice size.

Considering two-meson states with total momentum zero and without interaction, their energies are just the sum of the individual particle energies

$$E_{M_1(\mathbf{n})M_2(-\mathbf{n})}^{n.i.} = E_1(p) + E_2(p), \quad p = \frac{2\pi|\mathbf{n}|}{L}, \quad \mathbf{n} \in N^3. \quad (1)$$

In the presence of interactions, the energies get shifted depending on the interaction strength. For our lattice

setting the noninteracting two-meson levels with $J^{PC} = 1^{++}$, total momentum zero in the indicated energy range are

- $I = 0$; $\bar{c}c(\bar{u}u + \bar{d}d)$ and $\bar{c}c$; $E \lesssim 4.2$ GeV

$$\begin{array}{lll} D(0)\bar{D}^*(0), & J/\psi(0)\omega(0), & D(1)\bar{D}^*(-1), \\ J/\psi(1)\omega(-1), & \eta_c(1)\sigma(-1), & \chi_{c1}(0)\sigma(0). \end{array}$$

- $I = 1$; $\bar{c}c\bar{d}u$; $E \lesssim 4.2$ GeV

$$\begin{array}{lll} D(0)\bar{D}^*(0), & J/\psi(0)\rho(0), & D(1)\bar{D}^*(-1), \\ J/\psi(1)\rho(-1), & \chi_{c1}(1)\pi(-1), & \chi_{c0}(1)\pi(-1). \end{array}$$

- $I = 0$; $\bar{c}c\bar{s}s$ and $\bar{c}c$; $E \lesssim 4.3$ GeV

$$\begin{array}{lll} D_s(0)\bar{D}_s^*(0), & J/\psi(0)\phi(0), & D_s(1)\bar{D}_s^*(-1), \\ J/\psi(1)\phi(-1). \end{array}$$

The parentheses denote meson momenta in units of $2\pi/L$.

We consider the flavor sectors $\bar{c}c(\bar{u}u + \bar{d}d)$ and $\bar{c}c\bar{s}s$ separately. In nature these two $I = 0$ sectors can mix and they could in principle mix also in our simulation without dynamical strange quarks. However, if both flavor sectors would be treated together, then $6 + 4 = 10$ two-particle $I = 0$ states are expected below 4.2 GeV. This would make the resulting spectrum denser and noisier, so the identification of eigenstates and the search for exotics would be even more challenging. We therefore consider these two sectors separately in this first search for possible exotics in the extended energy region. The corresponding assumptions will be discussed for each flavor channel along with the results.

The noninteracting energies will be shown by the horizontal lines in our plots, and follow from the masses and the single meson energies determined on the same set of gauge configurations [24–26]. The energies of the σ meson using single-hadron approximation are $am_\sigma = 0.302(15)$ and $aE_{\sigma(1)} = 0.534(22)$. Including two-meson operators up to 4.2 GeV at $m_\pi = 266$ MeV should be sufficient in searching for narrow exotic candidates below 4.2 GeV. Details of all the interpolators used, including the diquark-antidiquark interpolators, can be found in the next section.

The mesons $R = \rho, \sigma$ are resonances that decay to $\pi\pi$ or $\pi\eta$ in QCD with $N_f = 2$. A proper simulation which would consider the three-meson system [27] has not been performed in practice yet. In absence of this, a simplifying approximation for channels containing these resonances is adopted. We determine the energy of $R(p)$ as the ground state energy obtained from the correlation matrix with $\sum_x e^{ipx} \bar{q}(x)\Gamma q(x)$ interpolators. This energy is used for the horizontal lines in the plots. This basis renders in all cases just one low-lying state. Within our approximation this low-lying state corresponds to a resonance R with momentum p , to a two-particle state $\pi\pi/\pi\eta$ with total momentum p , or to some mixture of R and

the two-particle state. We also do not consider nonresonant three-meson levels which could appear above $\eta_c\pi\pi$, $J/\psi\pi\pi$, $\eta_c K\bar{K}$, $J/\psi K\bar{K}$ thresholds. Based on the experience with two-meson operators we do not expect that without explicit incorporation of three-meson interpolating fields these three-meson states appear in the spectra.

III. LATTICE METHODOLOGY

These calculations are performed on $N_f = 2$ dynamical gauge configurations with $m_\pi \simeq 266$ MeV [28] and with other parameters provided in Table I. The mass-degenerate u/d quarks are based on a tree-level improved Wilson-clover action. The strange quark is present only in the valence sector and we assume that the valence strange content could uncover hints on the possible existence of the $\bar{c}c\bar{s}s$ exotics. The absence of dynamical strange quarks prevents $\bar{c}c\bar{s}s$ intermediate states in the $\bar{c}c(\bar{u}u + \bar{d}d)$ and $\bar{c}c$ sector, in accordance with treating these two $I = 0$ sectors separately in our study. With

a rather small box size of $L \simeq 2$ fm, one expects to have large finite size effects. On the other hand this serves as a crucial practical advantage by reducing the number of two-meson scattering states $M_1(\mathbf{n})M_2(-\mathbf{n})$ in the energy range of our interest. This helps in easier identification of the possible resonances that could exist along with the regular two-meson energy levels. It also reduces computational cost as one needs to consider a smaller number of distillation eigenvectors and two-meson interpolators with respect to a study in larger volume.

Lattice size	κ	β	N_{cfgs}	m_π [MeV]	a [fm]	L [fm]
$16^3 \times 32$	0.1283	7.1	280	266(3)(3)	0.1239(13)	1.98

TABLE I. Details of the gauge field ensemble used.

We construct altogether 22 interpolators with $J^{PC} = 1^{++}$ and total momentum zero for the three cases of our interest (T_1^{++} irreducible representation of the discrete lattice group O_h is employed):

$$\begin{aligned}
O_{1-8}^{\bar{c}c} &= \bar{c}\hat{M}c(0) \frac{1}{2}(1 + K_d), \quad \text{see Table X of Ref. [25]} \\
O_9^{MM} &= \bar{c}\gamma_5 u(0) \bar{u}\gamma_i c(0) - \bar{c}\gamma_i u(0) \bar{u}\gamma_5 c(0) + K_d\{u \rightarrow d\}, \\
O_{10}^{MM} &= \epsilon_{ijk} \bar{c}\gamma_j c(0) \{ \bar{u}\gamma_k u(0) + K_d\{u \rightarrow d\} \}, \\
O_{11}^{MM} &= \sum_{e_p=\pm e_{x,y,z}} \{ \bar{c}\gamma_5 u(e_p) \bar{u}\gamma_i c(-e_p) - \bar{c}\gamma_i u(e_p) \bar{u}\gamma_5 c(-e_p) \} + K_d\{u \rightarrow d\}, \\
O_{12}^{MM} &= \bar{c}\gamma_5 \gamma_4 u(0) \bar{u}\gamma_i \gamma_4 c(0) - \bar{c}\gamma_i \gamma_4 u(0) \bar{u}\gamma_5 \gamma_4 c(0) + K_d\{u \rightarrow d\}, \\
O_{13}^{MM} &= \epsilon_{ijk} \bar{c}\gamma_j \gamma_4 c(0) \{ \bar{u}\gamma_k \gamma_4 u(0) + K_d\{u \rightarrow d\} \}, \\
O_{14}^{MM} &= \sum_{e_p=\pm e_{x,y,z}} \epsilon_{ijl} \bar{c}\gamma_j c(e_p) \{ \bar{u}\gamma_l u(-e_p) + K_d\{u \rightarrow d\} \}, \\
O_{15}^{MM} &= \{ \bar{c}\gamma_5 c(e_p) \bar{u}u(-e_p) - \bar{c}\gamma_5 c(-e_p) \bar{u}u(e_p) \}_{p=i} + K_d\{u \rightarrow d\}, \\
O_{16}^{MM} &= \epsilon_{ijp} \{ \bar{c}\gamma_j \gamma_5 c(-e_p) \bar{u}\gamma_5 u(e_p) - \bar{c}\gamma_j \gamma_5 c(e_p) \bar{u}\gamma_5 u(-e_p) \} + K_d\{u \rightarrow d\}, \\
O_{17}^{MM} &= \bar{c}\gamma_i \gamma_5 c(0) \bar{u}u(0) + K_d\{u \rightarrow d\}, \\
O_{18}^{MM} &= \{ \bar{c}c(e_p) \bar{u}\gamma_5 u(-e_p) - \bar{c}c(-e_p) \bar{u}\gamma_5 u(e_p) \}_{p=i} + K_d\{u \rightarrow d\}, \\
O_{19}^{4q} &= [\bar{c} C \gamma_5 \bar{u}^T]_{3_c} [c^T \gamma_i C u]_{\bar{3}_c} + [\bar{c} C \gamma_i \bar{u}^T]_{3_c} [c^T \gamma_5 C u]_{\bar{3}_c} + K_d\{u \rightarrow d\}, \\
O_{20}^{4q} &= [\bar{c} C \bar{u}^T]_{3_c} [c^T \gamma_i \gamma_5 C u]_{\bar{3}_c} + [\bar{c} C \gamma_i \gamma_5 \bar{u}^T]_{3_c} [c^T C u]_{\bar{3}_c} + K_d\{u \rightarrow d\}, \\
O_{21}^{4q} &= [\bar{c} C \gamma_5 \bar{u}^T]_{\bar{6}_c} [c^T \gamma_i C u]_{6_c} + [\bar{c} C \gamma_i \bar{u}^T]_{\bar{6}_c} [c^T \gamma_5 C u]_{6_c} + K_d\{u \rightarrow d\}, \\
O_{22}^{4q} &= [\bar{c} C \bar{u}^T]_{\bar{6}_c} [c^T \gamma_i \gamma_5 C u]_{6_c} + [\bar{c} C \gamma_i \gamma_5 \bar{u}^T]_{\bar{6}_c} [c^T C u]_{6_c} + K_d\{u \rightarrow d\}.
\end{aligned} \tag{2}$$

The indices i, j, k and l define the Euclidean Dirac gamma matrices, while the index p indicates the momentum direction. Einstein's summation convention is implied for repeated indices. The unsummed index i in all the operators defines the polarization. The $C = i\gamma_2\gamma_4$ is the charge conjugation matrix. The coefficient K_d depends on the quark content: $K_d=1$ is used for $\bar{c}c(\bar{u}u + \bar{d}d)$ and $K_d=0$ for $\bar{c}c\bar{s}s$ followed by using strange quark propagators instead of the light quark propagators. For $I = 1$

channel we apply $K_d=-1$ which gives the flavor content $\bar{c}c(\bar{u}u - \bar{d}d)$ and has the same spectrum as $\bar{c}c\bar{d}u$ in the isospin limit.

We emphasize the use of four operators O^{4q} with diquark-antidiquark structure and color antitriplet or

N	$\bar{c}c(\bar{u}u + \bar{d}d)$	$\bar{c}c\bar{u}d$	$\bar{c}c\bar{s}s$
$O_{1-8}^{\bar{c}c}$	$\bar{c} \hat{M} c$	Does not couple	$\bar{c} \hat{M} c$
O_9^{MM}	$D(0)\bar{D}^*(0)$	$D(0)\bar{D}^*(0)$	$D_s(0)\bar{D}_s^*(0)$
O_{10}^{MM}	$J/\psi(0)\omega(0)$	$J/\psi(0)\rho(0)$	$J/\psi(0)\phi(0)$
O_{11}^{MM}	$D(1)\bar{D}^*(-1)$	$D(1)\bar{D}^*(-1)$	$D_s(1)\bar{D}_s^*(-1)$
O_{12}^{MM}	$D(0)\bar{D}^*(0)$	$D(0)\bar{D}^*(0)$	$D_s(0)\bar{D}_s^*(0)$
O_{13}^{MM}	$J/\psi(0)\omega(0)$	$J/\psi(0)\rho(0)$	$J/\psi(0)\phi(0)$
O_{14}^{MM}	$J/\psi(1)\omega(-1)$	$J/\psi(1)\rho(-1)$	$J/\psi(1)\phi(-1)$
O_{15}^{MM}	$\eta_c(1)\sigma(-1)$	$\eta_c(1)a_0(-1)$	Not used
O_{16}^{MM}	$\chi_{c1}(1)\eta(-1)$	$\chi_{c1}(1)\pi(-1)$	Not used
O_{17}^{MM}	$\chi_{c1}(0)\sigma(0)$	$\chi_{c1}(0)a_0(0)$	Not used
O_{18}^{MM}	$\chi_{c0}(1)\eta(-1)$	$\chi_{c0}(1)\pi(-1)$	Not used
O_{19-20}^{4q}	$[\bar{c}\bar{q}]_{3_c} [cq]_{\bar{3}_c}$	$[\bar{c}\bar{u}]_{3_c} [cd]_{\bar{3}_c}$	$[\bar{c}\bar{s}]_{3_c} [cs]_{\bar{3}_c}$
O_{21-22}^{4q}	$[\bar{c}\bar{q}]_{\bar{6}_c} [cq]_{6_c}$	$[\bar{c}\bar{u}]_{\bar{6}_c} [cd]_{6_c}$	$[\bar{c}\bar{s}]_{\bar{6}_c} [cs]_{6_c}$

TABLE II. List of interpolators ($J^{PC} = 1^{++}$) and their correspondence with various two-meson scattering channels.

sextet diquarks

$$[\bar{c}\Gamma_1\bar{q}]_G [c\Gamma_2q]_{\bar{G}} \equiv \sum_{\mathbf{x}_1} \mathcal{G}_{ab_1c_1} \bar{c}_{b_1}^{\alpha_1} \Gamma_1^{\alpha_1\beta_1} \bar{q}_{c_1}^{\beta_1}(\mathbf{x}_1, t_f) \cdot \sum_{\mathbf{x}_2} \mathcal{G}_{ab_2c_2} c_{b_2}^{\alpha_2} \Gamma_2^{\alpha_2\beta_2} q_{c_2}^{\beta_2}(\mathbf{x}_2, t_f). \quad (3)$$

Here $a = 1, 2, 3$ for color triplet and $a = 1, \dots, 6$ for sextet,

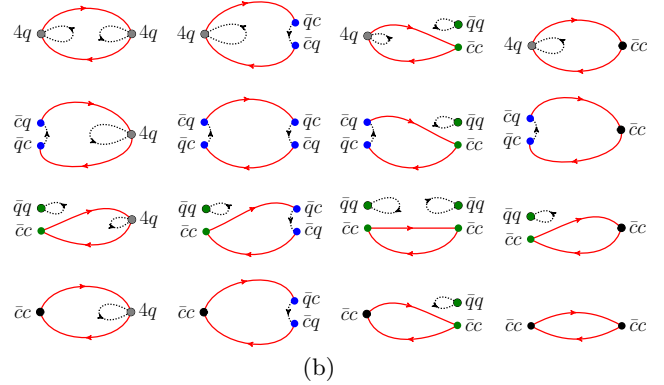
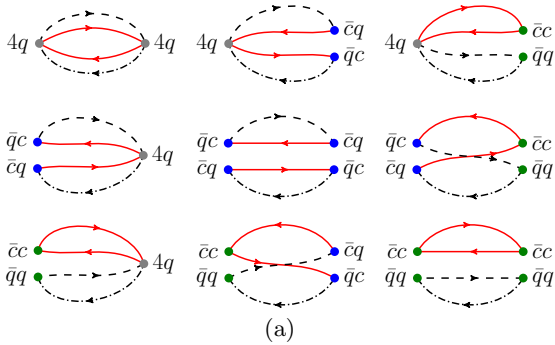


FIG. 1. The Wick contractions considered in our calculations. (a) Connected contraction diagrams. (b) Diagrams, in which the light/strange quarks do not propagate from source to sink. The correlation functions in the $\bar{c}c(\bar{u}u + \bar{d}d)$ and $\bar{c}c\bar{s}s$ cases are linear combinations of the diagrams of kind (a) and (b), while the correlation functions between the operators with quark content $\bar{c}c\bar{u}d$ are constructed purely from diagrams of kind (a).

Using the interpolators listed in Eq. (2) and Table II, we compute the full coupled correlation functions

$$\mathcal{C}_{jk}(t) = \langle \Omega | O_j(t_s + t) O_k^\dagger(t_s) | \Omega \rangle = \sum_n Z_k^{n*} Z_j^n e^{-E_n t}. \quad (5)$$

while $b, c = 1, 2, 3$ for both:

$$\begin{aligned} \mathcal{G}_{abc}^3 &= \mathcal{G}_{abc}^{\bar{3}} = \epsilon_{abc} \\ \mathcal{G}_{abc}^6 &= \mathcal{G}_{abc}^{\bar{6}} = 1 : a = 1, 2, 3 \text{ and } a \neq b \neq c \\ \mathcal{G}_{abc}^6 &= \mathcal{G}_{abc}^{\bar{6}} = \sqrt{2} : a = 4, 5, 6 \text{ and } a - 3 = b = c \end{aligned} \quad (4)$$

while the remaining \mathcal{G}_{abc} are zero. The operator [Eq. (3)] reduces to $\sum_{\mathbf{x}} \bar{c}(\mathbf{x})\bar{q}(\mathbf{x})c(\mathbf{x})q(\mathbf{x})$ on ensemble averaging, where the gauge configurations are not gauge fixed.

The interpolators are related with the two-meson channels as listed in Table II. noninteracting levels corresponding to some of these two-meson channels lie above our energy of interest, and the corresponding interpolators are not considered.

The Wick contractions considered in the computation of the correlation functions are shown in Figure 1. There are two other classes of diagrams, which are not considered: one in which no valence quark propagates from source to sink, and the other class in which only the light/strange quarks propagate from source to sink and the $\bar{c}c$ pair annihilates. The effects from these two classes of diagrams, with the charm quark not propagating from source to the sink, are known to be suppressed due to the Okubo-Zweig-Iizuka rule. They correspond to mixing with a number of channels that contain only the u/d and s quarks, which represents currently unsolved challenge in lattice QCD. Note that the annihilation of u/d and s quarks as well as mixing with $\bar{c}c$ is taken into account, unlike in the simulation [19] aimed at $Y(4140)$, for example.

For an efficient computation of these correlation matrices, we utilize the ‘‘distillation’’ method for the quark sources as proposed in Ref. [29]. In this method the quark sources are build from the N_v lowest eigenmodes of the gauge-covariant Laplacian on a given time slice, t_s .

We use $N_v=64$ for computation of correlators involving u/d quarks, while for the correlators with hidden strange content, we use $N_v=48$. The correlation functions with u/d quarks are computed only for polarization along the x -axis and averaged over all t_s , while correlation functions involving hidden strange quarks are averaged over all polarizations and for all even values of t_s .

The energies E_n and overlaps $Z_j^{(n)} = \langle \Omega | O_j | n \rangle$ for all eigenstates n are extracted using the well-established generalized eigenvalue problem [30]

$$\mathcal{C}(t) u^{(n)}(t) = \lambda^{(n)}(t, t_0) \mathcal{C}(t_0) u^{(n)}(t). \quad (6)$$

The energies E_n are extracted asymptotically from two-exponential fits to the eigenvalues

$$\lambda^{(n)}(t, t_0) \propto A_n e^{-E_n t} + A'_n e^{-E'_n t}, \quad E'_n > E_n. \quad (7)$$

We find consistent results for $t_0 = 2, 3$ and present the results for $t_0 = 2$. The two-exponential fits were typically done in the range $3 \leq t \leq 14$. The eigenvectors $u^{(n)}$ determine the overlaps

$$Z_j^{(n)}(t) = e^{E_n t/2} \frac{|\mathcal{C}_{jk}(t) u_k^{(n)}(t)|}{|\mathcal{C}(t) u^{(n)}(t)|}. \quad (8)$$

The statistical errors obtained using single-elimination jackknife analysis are quoted throughout.

The complete basis was used in the initial analysis, which was later reduced to an optimized basis, separately in each of the three cases, based on a systematic operator pruning. This procedure is aimed at getting better signals (in terms of the numbers of states and the quality of the effective mass plateau and the overlap factors) in comparison with the spectrum extracted from the full set of operators. After finalizing the optimized set of two-meson interpolators, we fixed the $\bar{c}c$ and $[\bar{c}q]_{\mathcal{G}}[cq]_{\mathcal{G}}$ operators that give good signals for a maximum number of extractable states below 4.2 GeV. The optimized basis that we used for the three cases of quark content are

$$\begin{aligned} \bar{c}c(\bar{u}u + \bar{d}d) : & O_{1,3,5}^{\bar{c}c}, O_{9-12,14,15,17}^{MM}, O_{19,21}^{4q} \\ \bar{c}c\bar{u}d : & O_{9-16,18}^{MM}, O_{19,21}^{4q} \\ \bar{c}c\bar{s}s : & O_{1,5}^{\bar{c}c}, O_{9-11,14}^{MM}, O_{19,21}^{4q}. \end{aligned} \quad (9)$$

Our principal aim is to find out whether QCD supports exotic states in addition to the conventional charmonia and the two-meson scattering levels, which inevitably appear in dynamical QCD. Analytic techniques have been proposed for the determination of the scattering matrix for coupled two-hadron scattering channels based on Lüscher-type finite volume formalisms [31]. These would in principle allow extraction of the masses and decay widths for resonances of interest. A number of lattice calculations have already dealt with resonances and shallow bound states in the elastic scattering (see

[32] and [33] for an example of each). The first calculation of a scattering matrix for two coupled channels also promises progress in this direction [34]. However, such an analysis is beyond the scope of current lattice simulations for more than two coupled channels and/or three-hadron scattering channels, which applies to the case considered.

Therefore we take a simplified approach, where the existence of possible exotic states is investigated by analyzing the number of energy levels, their positions and overlaps with the considered lattice operators $\langle \Omega | O_j | n \rangle$. The formalism does predict an appearance of a level in addition to the (shifted) two-particle levels if there is a relatively narrow resonance in one channel. We have, for example, found additional levels related to the resonances ρ [26], $K^*(892)$ [35], $D_0^*(2400)$ [25], and the bound state $D_{s0}^*(2317)$ [33]. Additional levels related to $K_0^*(1430)$ [34] and $X(3872)$ [17] have been found in the simulations of two coupled channels. Based on this experience, we expect an additional energy level if an exotic state is of similar origin, i.e. if it corresponds to a pole of the scattering matrix near the physical axis.

Consider a noninteracting situation. Several two-meson operators considered in Table II contain the vector meson $V(1)$ with one unit of momentum. This can reside in irreducible representations (irreps) A_1 or E_2 of the corresponding symmetry group Dic_4 [36, 37]. One expects two degenerate energy levels for $P(1)V(-1)$ since there are two ways to combine the vector-meson irrep (A_1, E_2) with the pseudoscalar-meson irrep (A_2) to obtain the rest frame irrep of interest T_1^+ (see Table III of [36]). The underlying reason is that PV state with $J^P = 1^+$ can be in s -wave or in d -wave (also in continuum) [38–40]. In the limit of small coupling between s - and d -wave, one energy level is due solely to the s -wave and the other one to d -wave [39, 40].¹ We implement only the s -wave interpolator $O^{P(1)V(-1)}$ [Eq. (2)] and therefore expect to see only one energy level; this is verified in our observed spectra shown in Sect. V. One would need to employ two distinct interpolators in order to find two $P(1)V(-1)$ energy levels, but the extraction of such eigenstates has not been attempted yet for two-meson systems in QCD to our knowledge. Our two-meson operators contain also $V_1(1)V_2(-1)$, where three levels are expected based on analogous arguments [36]; we expect to find only one level related to s -wave interpolators [Eq. (2)], and indeed we do not find two other levels related to d -wave (for total spins $S = 1, 2$). We emphasize that the omission of additional interpolator structures and avoidance of levels related to d -waves makes the search for possible exotics within our approach less cumbersome and results

¹ The PV spectrum resembles (in the noninteracting limit) the spectrum in the deuterium channel pn , since $S = 1$, $J^P = 1^+$ and $l = 0, 2$ apply in both cases. Figure 2 of [39] indicates that one level $n(1)p(-1)$ is related mostly to s -wave and the other to d -wave. Lüscher's quantisation condition [38] does not depend on the spins of the individual particles, but on their total spin S .

more transparent.²

Charm quarks being heavy are subject to large discretization errors. We treat the charm quarks using the Fermilab formulation [41], according to which we tune the charm quark mass by equating the spin averaged kinetic mass of the $1S$ charmonium to its physical value. With this formulation, the discretization errors are highly suppressed in the energy splitting $E_n - m_{s.a.}$, $m_{s.a.} = \frac{1}{4}(m_{\eta_c} + 3m_{J/\psi})$, which will be compared with the experiments. We utilized this method in our earlier calculations on this ensemble and found good agreement with the experiments for conventional charmonium in Ref. [25] as well as, for masses and widths of charmed mesons in Refs. [25, 33, 42].

IV. FIERZ RELATIONS

The diquark-antidiquark operators $[\bar{c}q]_{3_c}[cq]_{\bar{3}_c}$ and $[\bar{c}q]_{\bar{6}_c}[cq]_{6_c}$ can be expressed as linear combinations of color singlet currents $(\bar{c}c)_{1_c}(\bar{q}q)_{1_c}$ and $(\bar{c}q)_{1_c}(\bar{q}c)_{1_c}$ [14, 43]. These relations are obtained for local currents via Fierz rearrangement [44] and are presented in the Appendix. Note that our quarks are smeared and each meson in O^{MM} has definite momentum, but the Fierz relation suggests that O^{4q} and O^{MM} are still linearly dependent.

The Fierz rearrangement is the key idea behind Coleman's argument [45] that in the large N_c limit application of Fermion quadrilinears to the vacuum creates meson pairs and nothing else. In the physical world with $N_c=3$, it is argued that tetraquarks could exist at subleading orders [46] of large N_c QCD. However, in the presence of the leading order two-meson terms, one should take caution in interpreting the nature of the levels purely based on their overlap factors onto various four-quark interpolators.

Let us consider a comparative study between the lattice correlators and the Fierz expansion of O^{4q} operators. From Eq. (A5), we see that the first and second terms in the Fierz expansion represent DD^* , while the seventh term is similar to the $O_{17}^{MM} = \chi_{c1} \sigma$. Hence we expect significant correlations between these operators. This is indeed verified in Figure 2, showing the time averaged normalized ensemble averaged correlation matrix

$$\tilde{C}_{ij} = \frac{1}{9} \sum_{t=2}^{10} \frac{\bar{C}_{ij}(t)}{\sqrt{\bar{C}_{ii}(t)\bar{C}_{jj}(t)}}. \quad (10)$$

With this normalization all the diagonal entries are forced to unity and all the off-diagonal entries to be less

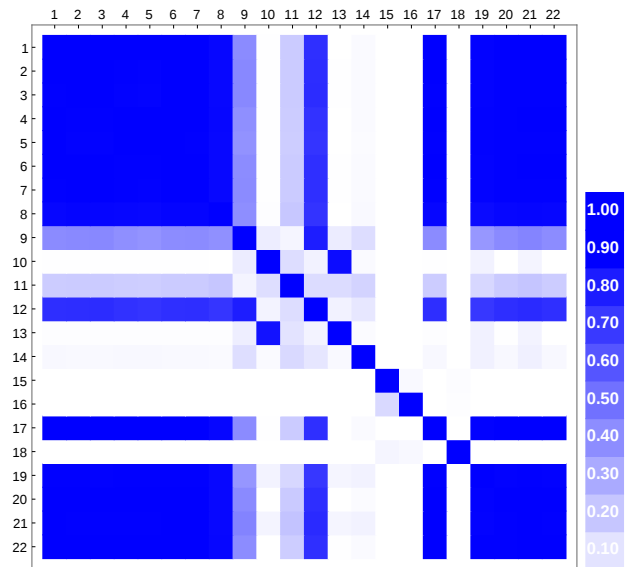


FIG. 2. Time averaged normalized correlation matrix \tilde{C} [Eq. (10)] for the operator basis O_{1-22} with quark content $\bar{c}c(\bar{u}u + \bar{d}d)$ and $\bar{c}c$. The axis ticks correspond to the order of operators used in Eq. (2).

than unity. The $[\bar{c}q]_{\bar{6}_c}[cq]_{6_c} = O_{19-22}^{4q}$ have large correlations onto the $DD^* = O_{9,11,12}^{MM}$ and $\chi_{c1} \sigma = O_{17}^{MM}$. The strong correlations between O^{4q} and O^{cc} operators can also be explained by the $\chi_{c1} \sigma$ component in O^{4q} , where σ couples to the vacuum.

V. RESULTS

The discrete spectra in Figs. 3 and 4 are the main results from our lattice calculation. They show the energies

$$E_n = E_n^{lat} - m_{s.a.}^{lat} + m_{s.a.}^{exp}, \quad m_{s.a.} = \frac{1}{4}(m_{\eta_c} + 3m_{J/\psi}) \quad (11)$$

of the states with $J^{PC} = 1^{++}$ and three quark contents. The horizontal lines represent various two-meson noninteracting energies.

The states that have dominant overlap with two-meson scattering operators are represented by circles and the color coding identifies the respective scattering channels based on the following criteria:

- The levels appear close to the expected two-meson noninteracting energies.
- They have dominant overlaps $\langle \Omega | O_j^{M_1 M_2} | n \rangle$ with corresponding $O_j^{M_1 M_2}$. This is also verified based on the ratios $Z_j^n / \max_m(Z_j^m)$, which are independent of normalization of operators and are shown in Figure 6.
- If the corresponding two-meson interpolators are excluded from the basis, this eigenstate disappears

² If one would find an extra state near $V(1)P(-1)$ or $V_1(1)V_2(-1)$, one would indeed have to identify whether this extra state arises due to the presence of the d -wave or is related to exotics. We do not address this question since we do not find such an extra state.

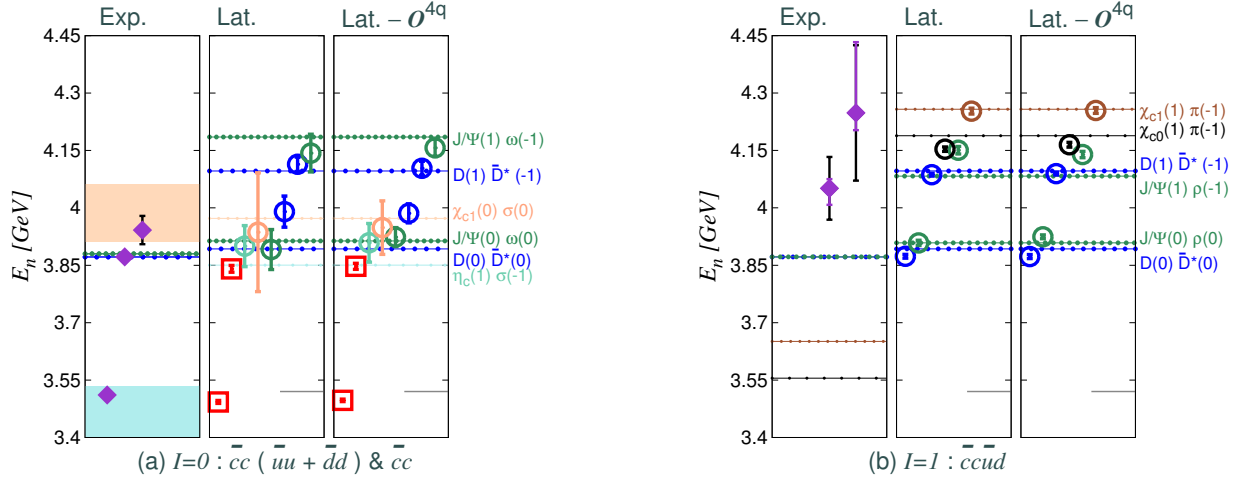


FIG. 3. The spectra of states with $J^{PC} = 1^{++}$ for the cases with u/d valence quarks. The energies $E_n = E_n^{lat} - m_{s.a.}^{lat} + m_{s.a.}^{exp}$ [Eq. (11)] are shown. The horizontal lines show energies of noninteracting two-particle states (1) and experimental thresholds, indicating uncertainty related to σ width. In each subplot, the middle block shows the discrete spectrum determined from our lattice simulation from the optimized basis [Eq. (9)]. The right-hand block shows the spectrum we obtained from the optimized basis of operators with the $[\bar{c}\bar{q}]_{\bar{g}}[cq]_{\bar{g}}$ operators excluded. The gray marks, on the right-hand side of each pane, indicate the lowest three-meson threshold $m_{\eta_c} + 2m_{\pi}$, while the actual lowest $\eta_c\pi\pi$ level on the lattice appears higher due to $l = 1$, which requires relative momenta. The left-hand block shows the physical thresholds and possible experimental candidates (a) χ_{c1} , $X(3872)$ and $X(3940)$, (b) $Z_c^+(4050)$ and $Z_c^+(4250)$. The violet error bars for experimental candidates show the uncertainties in the energy and the black error bars show its width.

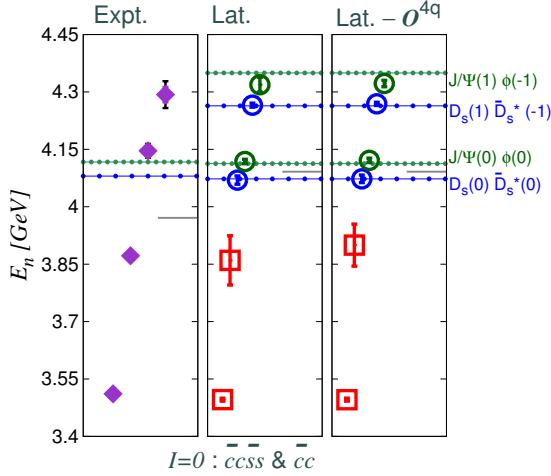


FIG. 4. The spectrum of states with $J^{PC} = 1^{++}$ and hidden strange quarks. The possible experimental candidates shown are χ_{c1} , $X(3872)$, $Y(4140)$ and $Y(4274)$. The gray marks, on the right-hand side of each pane, indicate the lowest three-meson threshold $m_{\eta_c} + 2m_K$. However, the actual lowest $\eta_c KK$ level on the lattice appears higher due to $l = 1$, which requires relative momenta. For further details see Figure 3.

or becomes too noisy to be identified. This is determined by comparing the pattern of the effective masses and overlaps between the original basis and the basis after operator exclusion.

The remaining states, that are not attributed to the two-meson scattering channels, are represented by red

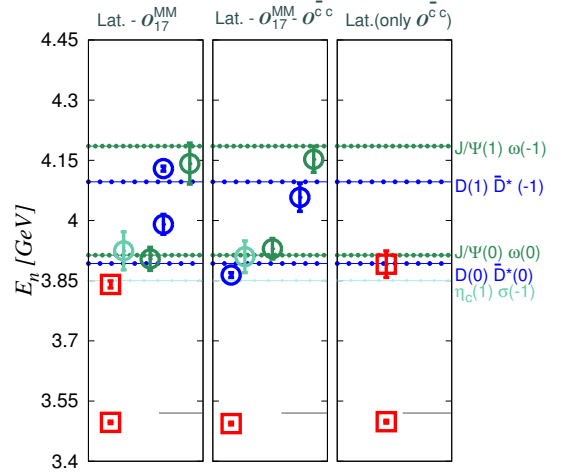


FIG. 5. The spectrum of states (Eq. (11)) with $J^{PC} = 1^{++}$ and quark content $\bar{c}c(\bar{u}u + \bar{d}d)$ & $\bar{c}c$. (i) Optimized basis (without O_{17}^{MM}), (ii) optimized basis without $\bar{c}c$ operators (and without O_{17}^{MM}) and (iii) basis with only $\bar{c}c$ operators. Note that candidate for $X(3872)$ disappears when removing $\bar{c}c$ operators although diquark-antidiquark operators are present in the basis, while it is not clear to infer on the dominant nature of this state just from the third panel. The $O_{17}^{MM} = \chi_{c1}(0)\sigma(0)$ is excluded from the basis to achieve better signals and clear comparison.

squares.

Figures 3 and 4 also compare the spectra between the two bases of operators, one with optimized operator set and another with the optimized set excluding $[\bar{c}\bar{q}]_{\bar{g}}[cq]_{\bar{g}}$.

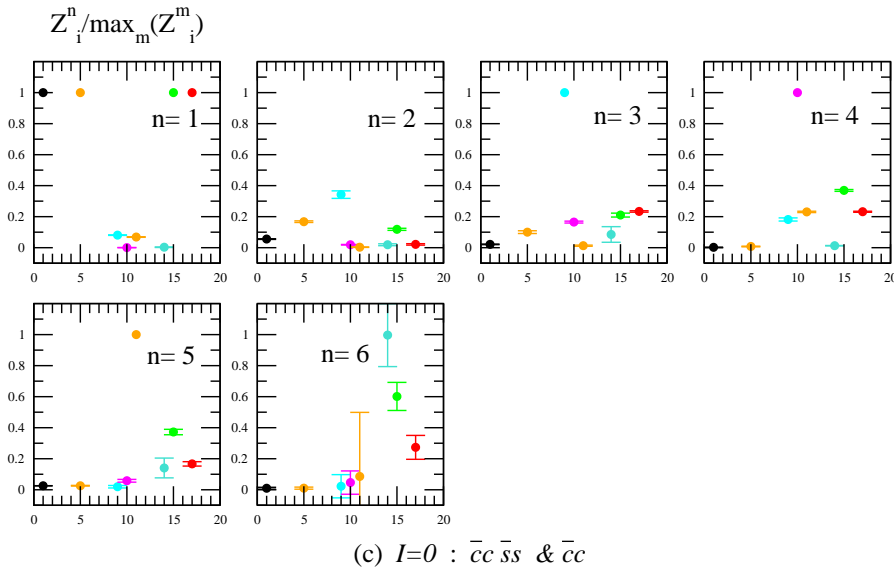
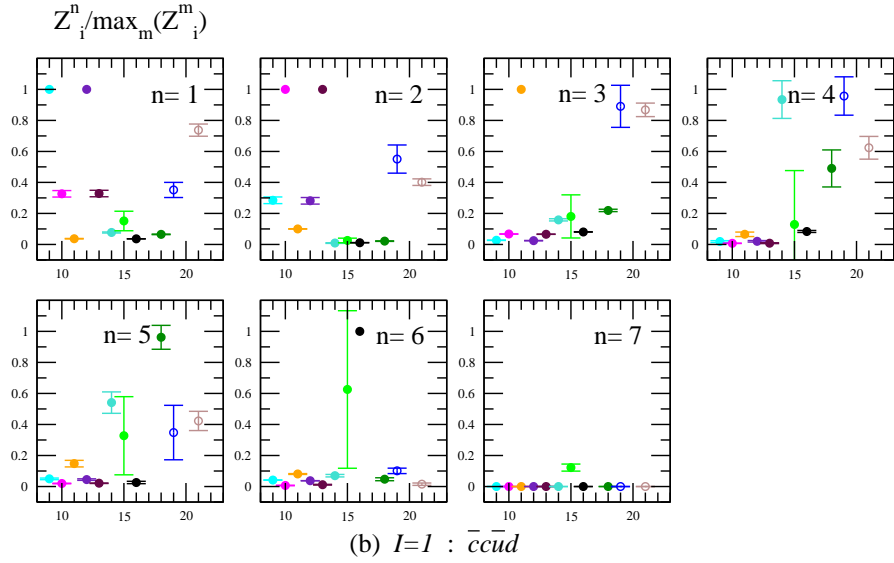
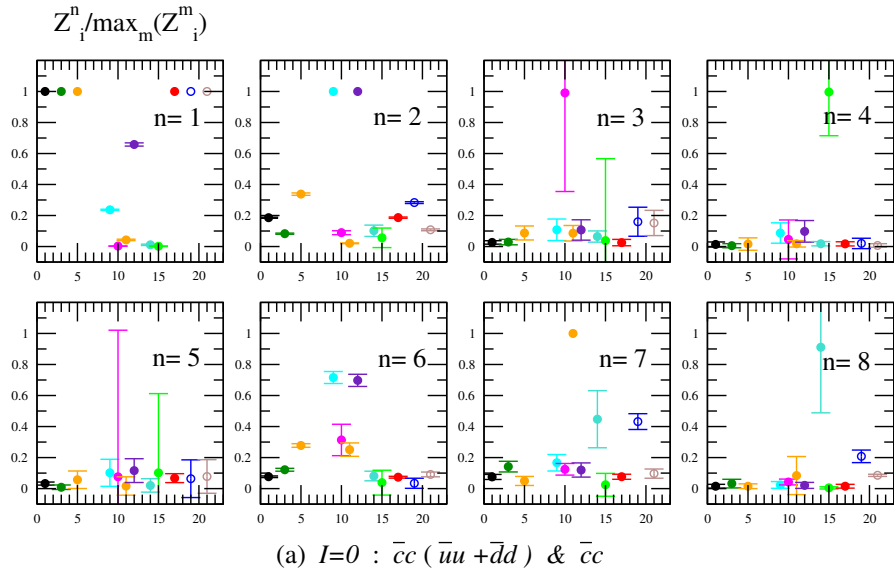


FIG. 6. The overlap factors $Z_j^{(n)} = \langle \Omega | O_j | n \rangle$ [Eq. (8)] shown in units of the maximal $|Z_j^m|$ for a given operator j across all the eigenstates m . These ratios are independent of the normalization of the interpolators O_j . The horizontal axis corresponds to the complete basis of interpolators [Eq. (2)], where the optimized subsets [Eq. (9)] were employed. The levels are ordered from lowest to highest E_n as in the middle pane of the spectrum in Figs. 3 and 4. The values are averages of the ratios over $4 \leq t \leq 13$ with error bars due to jackknife sampling.

In all three cases we see an almost negligible effect on the low lying states, while we do observe an improvement in the signals for higher lying states in the basis without $[\bar{c}\bar{q}]_{\bar{G}}[cq]_G$. The same conclusion applies for overlaps.

The employed irreducible representation T_1^{++} contains the states $J^{PC} = 1^{++}$ of interest, as well as $J^{PC} = 3^{++}$ states due to the broken rotational symmetry. Upon inclusion of the interpolator $O_8^{\bar{c}c}$ to the basis [Eq. (9)] the spectra for both $I = 0$ channels remain essentially unchanged except for an additional level at $E \simeq 4.1 - 4.2$ GeV [Eq. (11)]. This is where the earlier simulation on the same ensemble [25] and the simulation [47] have identified the only 3^{++} state in the energy region of our interest. In the following subsections, we present the spectra of $J^{PC} = 1^{++}$ states in three flavor channels for the basis (Eq. (9)), where $O_8^{\bar{c}c}$ is excluded.

A. $I = 0$ channel with flavor $\bar{c}c(\bar{u}u + \bar{d}d)$ and $\bar{c}\bar{c}$

This is the channel where the experimental $X(3872)$ resides. We will argue that the energy levels affected by this state are $n = 2$ (red squares) and $n = 6$ (blue circle) from Figure 3(a). The lowest state is the conventional $\chi_{c1}(1P)$. The overlaps of the three low-lying levels represented by circles show dominant $J/\psi(0)\omega(0)$, $\eta_c(1)\sigma(-1)$ and $\chi_{c1}(0)\sigma(0)$ Fock components. The highest two states in Figure 3(a) have significant overlap with the $J/\psi(1)\omega(-1)$ and $D_0(1)\bar{D}_0^*(-1)$ operators.

Now we focus on the eigenstates that are related to $X(3872)$. The $\bar{c}c$ interpolators alone give an eigenstate close to $D\bar{D}^*$ threshold (right pane of Figure 5), but one cannot establish whether this eigenstate is related to $X(3872)$ or to nearby two-meson states in this case. Therefore we turn to the spectrum of the full optimized basis [midpane in Figure 3(a)], where levels $n = 2$ (red squares) and $n = 6$ (blue circles) are found to have dominant overlap with the $\bar{c}c$ and $D\bar{D}^*$ operators. Excluding either of these operators results in disappearance of one level and a shift in the other level towards the $D\bar{D}^*$ threshold. We emphasize that one of the two levels remains absent when $D\bar{D}^*$ and O^{4q} are used and $O^{\bar{c}c}$ is not, as is evident from the first and second panel from the left of Figure 5. This indicates that the $\bar{c}c$ Fock component is crucial for $X(3872)$, while the $[\bar{c}\bar{q}]_{\bar{G}}[cq]_G$ structure alone does not render it. This also implies a combined dominance of $\bar{c}c$ and $D\bar{D}^*$ operators in determining the position of these two levels, while their resulting energies are not significantly affected whether O^{4q} is used in addition or not.

We determine the $D\bar{D}^*$ scattering phase shift from levels $n = 2, 6$ via Lüscher's relation [31] assuming elastic scattering. The phase shift is interpolated near threshold using the effective-range approximation. The eigenstate $n = 6$ (blue circle) is interpreted as the $D(0)\bar{D}^*(0)$ scattering state, which is significantly shifted up due to a large negative scattering length [48]. The resulting scattering matrix $T \propto 1/(\cot \delta(p) - i)$ has a pole just below

$X(3872)$	$m_X - m_{s.a.}$	$m_X - m_{D_0} - m_{D_0^*}$
Lat.	816(15)	-8(15)
Lat. - O^{4q}	815(8)	-9(8)
LQCD [17]	815(7)	-11(7)
LQCD [18]	-	-13(6)
Exp.	803(1)	-0.11(21)

TABLE III. Mass of $X(3872)$ with respect to $m_{s.a.}$ and the $D_0\bar{D}_0^*$ threshold. Our estimates are from the correlated fits to the corresponding eigenvalues using single exponential fit form with and without diquark-antidiquark operators. Results from previous lattice QCD simulations [17, 18] and experiment are also presented.

the threshold where $\cot \delta(p_B) = i$ is satisfied. We neglect possible effects of the left-hand cut in the partial wave amplitude. The results confirm a shallow bound state just below the $D\bar{D}^*$ threshold and the binding momentum p_B renders the mass of the bound state, interpreted as experimentally observed $X(3872)$. The resulting mass of $X(3872)$ and its binding energy are provided in Table III and in Figure 7, which indicate that it is insensitive to inclusion of diquark-antidiquark interpolators within errors. The mass of $X(3872)$ was extracted along these lines for the first time in Ref. [17], where this channel was studied in a smaller energy range on the same ensemble without diquark-antidiquark interpolators. The error on the binding energy in the present paper is larger due to the larger interpolator basis. These results are in agreement with a possible interpretation of $X(3872)$, where its properties are due to the accidental alignment of a $\bar{c}c$ state with the $D^0\bar{D}^{*0}$ threshold [49, 50], but we cannot rule out other options.

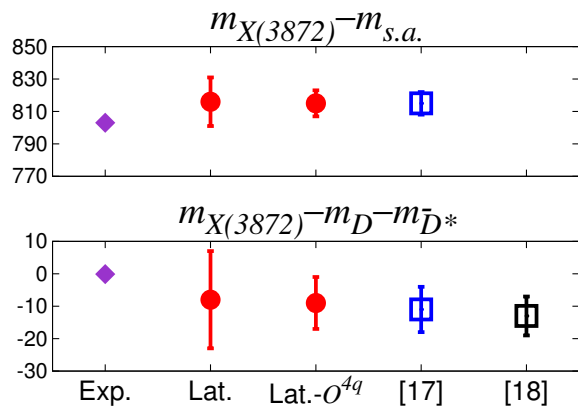


FIG. 7. Mass of $X(3872)$ with respect to $m_{s.a.}$ from the present simulation, previous lattice studies [17, 18] and experiment [6].

With regard to the other experimentally observed charmonia-like states [e.g. $X(3940)$], which could appear in this channel, we do not find any candidate in addition to the expected two-meson scattering levels. We also do not find candidates for other $\bar{c}c$ states with $J^{PC} = 1^{++}$

[e.g. $\chi_{1c}(nP)$] in the region between the $D\bar{D}^*$ threshold and 4.2 GeV.

B. $I = 1$ channel with flavor $\bar{c}c\bar{d}u$

A careful analysis of this isospin channel is crucial due to the large branching ratio for the decay $X(3872) \rightarrow J/\psi\rho$ and current experimental interests in search of a charged $X(3872)$. With no disconnected diagrams allowed in the light quark propagation, the correlation matrix is constructed purely of four-quark interpolators and connected Wick contractions in Figure 1(a).

The spectrum of eigenstates is shown in Figure 3(b), where all energies are close to noninteracting energy levels. All the eigenstates have a dominant overlap with the two-meson interpolators. The spectrum shows very little influence on the inclusion of $[\bar{c}\bar{q}]_{\mathcal{G}}[cq]_{\mathcal{G}}$, which is evident from Figure 3(b). Given that all the levels below 4.2 GeV can be attributed to the expected two-meson scattering states, we conclude that our lattice simulation gives no evidence for $Z_c(4050)^+$ and $Z_c(4250)^+$.

Our results also do not support charged or neutral $X(3872)$ with $I = 1$. There is no experimental indication for charged X , while the neutral X does have a large decay rate to $I = 1$ final state $J/\psi\rho^0$. One popular phenomenological explanation for this decay is that $X(3872)$ has $I = 0$ and the isospin is broken in the decay mechanism (due to the $D^+\bar{D}^{*-}$ vs $D^0\bar{D}^{*0}$ mass difference) [50, 51]. According to another explanation, X is a linear combination of $I = 0$ and $I = 1$ components, where the $I = 1$ component vanishes in the isospin limit [52]. Our simulation is performed in the isospin limit $m_u = m_d$, so it is perhaps not surprising that X with $I = 1$ is not observed. Future simulations with nondegenerate u/d quarks would be very welcome for this channel.

As pointed out in Section II, ρ in $J/\psi\rho$ is treated as stable, although $\rho(1)$ is kinematically close to the decay channel $\pi(1)\pi(0)$. In the absence of a simulation of a three-meson system, it is disputable what ‘noninteracting’ energy should be taken for the $\rho(1)$. An estimate from the diagonal correlator $\rho(1)$ leads to ‘noninteracting’ energy roughly 65 MeV below the eigenstate energy, which is identified to have a dominant overlap with the $J/\psi(1)\rho(-1)$ interpolator. However, taking the resonance position [26] brings the ‘noninteracting’ level in agreement with the measured eigenenergy.

C. $I = 0$ channel with flavor $\bar{c}c\bar{s}s$ and $\bar{c}c$

Our goal in simulating this channel is to search for a possible presence of the $Y(4140)$ resonance, which was found in $J/\psi\phi$ scattering in several experiments [10]. Our lattice simulation of $J/\psi\phi$ scattering takes into account the annihilation of the valence strange quarks and thereby the mixing with $\bar{c}c$ flavor content.

With no strange quark effects in the sea, the study of this channel is based on the following assumptions. We construct a basis with only $\bar{c}c$ and four-quark operators (O^{MM}, O^{4q}) with valence hidden strange content for this analysis. We assume that these interpolators have negligible coupling to two-meson states with flavor content $\bar{c}c(\bar{u}u + \bar{d}d)$. In other words, we assume that two-meson states like $D\bar{D}^*$ and $J/\psi\omega$ will not appear in the spectrum based on the chosen interpolators. The resulting spectrum in this channel confirms this assumption. We point out that $Y(4140)$ has been experimentally observed only in the $J/\psi\phi$ final state with valence strange content, but it has not been observed in $D\bar{D}^*$ and $J/\psi\omega$ final states. Although this ensemble does not have strange quarks in the sea, we assume that the valence strange content could uncover hints on the existence of the charm-strange exotics, if they exist.

Spectra in this channel are shown in Figure 4. We identify the lowest two states, represented by squares, to be $\chi_{c1}(1P)$ and the level related to $X(3872)$. The remaining four states are identified with the expected $D_s\bar{D}_s^*$ and $J/\psi\phi$ scattering levels. Thus in the energy region below 4.2 GeV, we find no levels that could be related to $Y(4140)$ or any other exotic structure. Note that the existence of $Y(4140)$ is not yet finally settled from experiment, and its quantum numbers, except for $C = +1$, are unknown. Therefore it is possible that its absence in our simulation is related to the fact that we explored the channel $J^P = 1^+$ only.

D. Discussion

The only exotic charmonium-like state found in our simulation is a $X(3872)$ candidate with $J^{PC} = 1^{++}$ and $I = 0$. It is found as a bound state slightly below $D\bar{D}^*$ threshold and has a mass close to the experimental mass of $X(3872)$. We point out that this mass corresponds to our $m_\pi \simeq 266$ MeV and was obtained from a rather small lattice volume, while chiral and continuum extrapolations have not been performed. Precision determination of its mass with respect to $D\bar{D}^*$ threshold will be a challenging task for future lattice simulation on larger volumes, which also should account for its coupling with multiple open scattering channels involving two or more hadrons. Recent analytic studies consider the quark mass dependence, the volume dependence and the effect from the isospin breaking relevant for future lattice studies of $X(3872)$ [53].

Candidates for no other ‘exotic’ charmonium-like states [except for $X(3872)$] are found in our exploration of the three $J^{PC} = 1^{++}$ channels. We list several possible reasons for the absence of the energy levels related to other possible exotic states in our simulation:

- The existence of $Y(4140)$, $Z_c^+(4050)$, $Z_c^+(4250)$ or any other exotic state in these channels, is not yet settled experimentally. Even if they exist, only $C =$

+1 is established experimentally, while their J^P is unknown. This could explain their absence in our simulation, which probes only $J^P = 1^+$.

- Based on the experience, discussed in Section III, we expect an additional energy level if the exotic state is a resonance associated to a pole near the real axis in the unphysical Riemann sheet. The absence of an additional energy level could also indicate a different origin of the experimental peak, e.g., a coupled-channel threshold effect. Further analytical work and lattice simulations are needed to settle the question whether an additional energy level is expected in this case.
- Finally, we cannot exclude the possibility that some exotic candidates could be absent due to the relatively heavy pion mass $m_\pi \simeq 266$ MeV, isospin limit $m_u = m_d$, neglect of the charm annihilation contributions, or the absence of the strange dynamical quarks in our simulation.

VI. CONCLUSIONS

We present the spectra from a lattice QCD simulation of $J^{PC} = 1^{++}$ channels with three different quark contents: $\bar{c}c\bar{d}u$, $\bar{c}c(\bar{u}u + \bar{d}d)$ and $\bar{c}c\bar{s}s$, where the later two can mix with $\bar{c}c$. The pion mass in this study with u/d dynamical quarks is $m_\pi \simeq 266$ MeV. Using a large number of interpolating fields $[\bar{c}\bar{q}]_{3_c}[cq]_{\bar{3}_c}$, $[\bar{c}\bar{q}]_{\bar{6}_c}[cq]_{6_c}$, $(\bar{c}q)_{1_c}(\bar{q}c)_{1_c}$, $(\bar{c}c)_{1_c}(\bar{q}q)_{1_c}$ and $(\bar{c}c)_{1_c}$, we extract the spectra up to 4.2 GeV. We find evidence for χ_{c1} and $X(3872)$, while all the remaining eigenstates are related to the expected two-meson scattering channels, which inevitably appear in the dynamical QCD. The $\bar{c}c$ Fock component in $X(3872)$ appears to be more important than the $[\bar{c}\bar{q}]_{\bar{6}_c}[cq]_{6_c}$, since we find a candidate for $X(3872)$ only when $\bar{c}c$ interpolating fields are used. The $D\bar{D}^*$ interpolators show a more prominent effect on the position of $X(3872)$ than the $[\bar{c}\bar{q}]_{\bar{6}_c}[cq]_{6_c}$. Candidates for charged or neutral $X(3872)$ with $I = 1$ are not found in our simulation with $m_u = m_d$, and future simulations with broken isospin would be welcome for this channel. We also do not find a candidate for $Y(4140)$ or any other exotic charmonium-like structure. Our search for the exotic states assumes an appearance of an additional energy eigenstate on the lattice, which is a typical manifestation for conventional hadrons. Further analytic work is needed to establish whether this working assumption applies also for several coupled channels and all exotic structures of interest.

ACKNOWLEDGMENTS

We thank Anna Hasenfratz and the PACS-CS for providing the gauge configurations. We acknowledge the discussions with R. Briceño, L. Leskovec, D. Mohler, S. Ozaki, S. Sasaki and C. DeTar. The calculations

were performed on computing clusters at the University of Graz (NAWI Graz), at the Vienna Scientific Cluster (VSC) and at Jozef Stefan Institute. This work is supported in part by the Austrian Science Fund FWF: I1313-N27 and by the Slovenian Research Agency ARRS Project No. N1-0020. S.P. acknowledges support from U.S. Department of Energy Contract No. DE-AC05-06OR23177, under which Jefferson Science Associates, LLC, manages and operates Jefferson Laboratory.

Appendix A: Fierz transformation of diquark-antidiquark operators

In this appendix we express the local diquark-antidiquark interpolator as

$$O^{4q}(x) = \sum F_i M_1^i(x) M_2^i(x) \quad (\text{A1})$$

using Fierz transformations [44], where

$$M(x) = \bar{q}_a \Gamma q'_a(x) \quad (\text{A2})$$

are local color-singlet currents. The momentum projected interpolator $O^{4q}(p)$ is then given by

$$\begin{aligned} O^{4q}(p) &= \sum_i F_i \sum_x e^{ipx} M_1^i(x) M_2^i(x) \\ &= \sum_i \frac{F_i}{V^2} \sum_x e^{ipx} \sum_q e^{-iqx} M_1^i(q) \sum_k e^{-ikx} M_2^i(k) \\ &= \sum_i \frac{F_i}{V} \sum_q M_1^i(q) M_2^i(p-q). \end{aligned}$$

Thus the projection to total momentum zero $O^{4q}(p=0)$ can be rewritten as sum over two-meson operators with back-to-back momenta.

Fierz transformation is an operation of rearranging the Fermion fields in a Fermion quadrilinear. Expressing our local diquark-antidiquark interpolator with explicit color (lower) indices and Dirac (upper) indices, we have

$$\begin{aligned} [\bar{c} P \bar{q}]_{\mathcal{G}} [c N q]_{\mathcal{G}} \Big|_{\binom{3_c}{6_c}} &= \mathcal{G}_{abc} \mathcal{G}_{ade} \bar{c}_b^\alpha P^{\alpha\beta} \bar{q}_c^{\beta} c_d^\eta N^{\eta\delta} q_e^\delta \\ &= (\delta_{bd} \delta_{ce} \mp \delta_{be} \delta_{cd}) P^{\alpha\beta} N^{\eta\delta} \bar{c}_b^\alpha \bar{q}_c^\beta c_d^\eta q_e^\delta \\ &= P^{\alpha\beta} N^{\eta\delta} \{ -(\bar{c}^\alpha c^\eta)_{1_c} (\bar{q}^\beta q^\delta)_{1_c} \mp (\bar{c}^\alpha q^\delta)_{1_c} (\bar{q}^\beta c^\eta)_{1_c} \} \\ &= -(\bar{c}^\alpha \Gamma_I^{\alpha\eta} c^\eta)_{1_c} (\bar{q}^\beta G_I^{\beta\delta} q^\delta)_{1_c} \mp (\bar{c}^\alpha \Gamma_I^{\alpha\delta} q^\delta)_{1_c} (\bar{q}^\beta H_I^{\beta\eta} c^\eta)_{1_c} \\ &= -(\bar{c} \Gamma_I c)_{1_c} (\bar{q} G_I q)_{1_c} \mp (\bar{c} \Gamma_I q)_{1_c} (\bar{q} H_I c)_{1_c} \quad (\text{A3}) \end{aligned}$$

where we have accounted for $\mathcal{G}_{abc} \mathcal{G}_{ade} \Big|_{\binom{3_c}{6_c}} = \delta_{bd} \delta_{ce} \mp \delta_{be} \delta_{cd}$ in the second line and a minus sign for Fermion exchange in the third. Each term on the right-hand side of the fourth line is expressed as a sum over the index $I = 1, \dots, 16$, where Γ_I are the elements of Clifford algebra $\{\Gamma\}$ and (G_I, H_I) the unknown coefficient matrices.

These coefficient matrices can be determined using the orthogonality relation $Tr[\Gamma_I \Gamma_J] = 4\delta_{IJ}$

$$G_I = \frac{1}{4}(N^T \Gamma_I P)^T \quad \text{and} \quad H_I = \frac{1}{4}(N \Gamma_I P)^T \quad (\text{A4})$$

The diquark-antidiquark fields can therefore be expressed as a linear combination of products of two color singlet currents with various Dirac structures. Local analogs of our diquark-antidiquark interpolating fields can be expressed as

$$\begin{aligned} O_{(19)}^{4q} &= [\bar{c} C \gamma_5 \bar{u}]_G [c \gamma_i C u]_G + [\bar{c} C \gamma_i \bar{u}]_G [c \gamma_5 C u]_G + K_d \{u \rightarrow d\} \\ &= \mp \frac{(-1)^i}{2} \{ (\bar{c} \gamma_5 u)(\bar{u} \gamma_i c) - (\bar{c} \gamma_i u)(\bar{u} \gamma_5 c) \\ &\quad + (\bar{c} \gamma^\nu \gamma_5 u)(\bar{u} \gamma_i \gamma_\nu c)|_{i \neq \nu} - (\bar{c} \gamma_i \gamma_\nu u)(\bar{u} \gamma^\nu \gamma_5 c)|_{i \neq \nu} \} \\ &\quad + \frac{(-1)^i}{2} \{ (\bar{c} c)(\bar{u} \gamma_i \gamma_5 u) + (\bar{c} \gamma_i \gamma_5 c)(\bar{u} u) \\ &\quad - (\bar{c} \gamma^\nu c)(\bar{u} \gamma_i \gamma_\nu \gamma_5 u)|_{i \neq \nu} - (\bar{c} \sigma^{\alpha\beta} c)(\bar{u} \sigma_{\alpha\beta} \gamma_i \gamma_5 u)|_{i \neq (\alpha < \beta)} \} \\ &\quad + K_d \{u \rightarrow d\} \end{aligned} \quad (\text{A5})$$

and

$$\begin{aligned} O_{(20)}^{4q} &= [\bar{c} C \bar{u}]_G [c \gamma_i \gamma_5 C u]_G + [\bar{c} C \gamma_i \gamma_5 \bar{u}]_G [c C u]_G + K_d \{u \rightarrow d\} \\ &= \mp \frac{(-1)^i}{2} \{ -(\bar{c} u)(\bar{u} \gamma_i \gamma_5 c) + (\bar{c} \gamma_i \gamma_5 u)(\bar{u} c) \\ &\quad - (\bar{c} \gamma^\nu u)(\bar{u} \gamma_i \gamma_\nu \gamma_5 c)|_{i \neq \nu} + (\bar{c} \sigma^{\alpha\beta} u)(\bar{u} \sigma_{\alpha\beta} \gamma_i \gamma_5 c)|_{i \neq (\alpha < \beta)} \} \\ &\quad - \frac{(-1)^i}{2} \{ (\bar{c} c)(\bar{u} \gamma_i \gamma_5 u) - (\bar{c} \gamma_i \gamma_5 c)(\bar{u} u) \\ &\quad + (\bar{c} \gamma^\nu c)(\bar{u} \gamma_i \gamma_\nu \gamma_5 u)|_{i \neq \nu} - (\bar{c} \sigma^{\alpha\beta} c)(\bar{u} \sigma_{\alpha\beta} \gamma_i \gamma_5 u)|_{i \neq (\alpha < \beta)} \} \\ &\quad + K_d \{u \rightarrow d\}. \end{aligned} \quad (\text{A6})$$

Various terms resemble two-meson operators O^{MM}

[Eq. 2], where $(\bar{q}\Gamma q')$ denote color singlet currents.

-
- [1] M. Ablikim *et al.* [BESIII Collaboration], Phys. Rev. Lett. **110**, 252001 (2013); Z. Q. Liu *et al.* [Belle Collaboration], Phys. Rev. Lett. **110**, 252002 (2013); T. Xiao *et al.*, Phys. Lett. B **727**, 366 (2013).
- [2] S. K. Choi *et al.* [BELLE Collaboration], Phys. Rev. Lett. **100**, 142001 (2008); K. Chilikin *et al.*, Phys. Rev. D **88**, no. 7, 074026 (2013); R. Aaij *et al.* [LHCb Collaboration], Phys. Rev. Lett. **112**, no. 22, 222002 (2014).
- [3] R. Mizuk *et al.* [BELLE Collaboration], Phys. Rev. D **80**, 031104 (2009).
- [4] S. K. Choi *et al.* [Belle Collaboration], Phys. Rev. Lett. **91**, 262001 (2003) [hep-ex/0309032].
- [5] R. Aaij *et al.* [LHCb Collaboration], Phys. Rev. Lett. **110**, 222001 (2013) [arXiv:1302.6269 [hep-ex]].
- [6] K. A. Olive *et al.* [Particle Data Group Collaboration], Chin. Phys. C **38**, 090001 (2014).
- [7] B. Aubert *et al.* [BaBar Collaboration], Phys. Rev. D **71**, 031501 (2005); S.-K. Choi, *et al.* [Belle Collaboration], Phys. Rev. D **84**, 052004 (2011).
- [8] K. Abe *et al.* [Belle Collaboration], Phys. Rev. Lett. **94**, 182002 (2005); B. Aubert *et al.* [BaBar Collaboration], Phys. Rev. Lett. **101**, 082001 (2008).
- [9] S. L. Olsen, Front. Phys. **10**, 101401 (2015); A. Esposito *et al.*, arXiv:1411.5997 [hep-ph]; N. Brambilla *et al.*, Eur. Phys. J. C **74**, no. 10, 2981 (2014); E. S. Swanson, Phys. Rept. **429**, 243 (2006); X. Liu, Chin. Sci. Bull. **59**, 3815 (2014).
- [10] T. Aaltonen *et al.* [CDF Collaboration], Phys. Rev. Lett. **102**, 242002 (2009), arXiv:1101.6058 [hep-ex]; S. Chartrchyan *et al.* [CMS Collaboration], Phys. Lett. B **734**, 261 (2014); V. M. Abazov *et al.* [D0 Collaboration], Phys. Rev. D **89**, no. 1, 012004 (2014); J. P. Lees *et al.* [BABAR Collaboration], Phys. Rev. D **91**, no. 1, 012003 (2015).
- [11] X. Liu, Z. G. Luo and S. L. Zhu, Phys. Lett. B **699**, 341 (2011) [Erratum-ibid. B **707**, 577 (2012)] [arXiv:1011.1045 [hep-ph]].
- [12] C. P. Shen *et al.* [Belle Collaboration], Phys. Rev. Lett. **104**, 112004 (2010) [arXiv:0912.2383 [hep-ex]].
- [13] E. S. Swanson, Phys. Lett. B **588**, 189 (2004) [hep-ph/0311229].
- [14] L. Maiani *et al.*, Phys. Rev. D **71**, 014028 (2005) [hep-ph/0412098].

- [15] D. V. Bugg, Phys. Rev. D **71**, 016006 (2005) [hep-ph/0410168].
- [16] F. E. Close and P. R. Page, Phys. Lett. B **578**, 119 (2004) [hep-ph/0309253].
- [17] S. Prelovsek and L. Leskovec, Phys. Rev. Lett. **111**, 192001 (2013) [arXiv:1307.5172 [hep-lat]].
- [18] S. H. Lee *et al.* [Fermilab Lattice and MILC Collaborations], arXiv:1411.1389 [hep-lat].
- [19] S. Ozaki and S. Sasaki, Phys. Rev. D **87**, no. 1, 014506 (2013) [arXiv:1211.5512 [hep-lat]].
- [20] R. L. Jaffe, Phys. Rev. D **15**, 281 (1977); R. L. Jaffe and F. E. Low, Phys. Rev. D **19**, 2105 (1979).
- [21] L. Maiani *et al.*, Phys. Rev. Lett. **93**, 212002 (2004), Phys. Rev. D **89**, no. 11, 114010 (2014); N. Barnea, J. Vijande and A. Valcarce, Phys. Rev. D **73**, 054004 (2006); J. Vijande *et al.*, Phys. Rev. D **76**, 094022 (2007), Phys. Rev. D **76**, 094027 (2007); T. Fernandez-Carames, A. Valcarce and J. Vijande, Phys. Rev. Lett. **103**, 222001 (2009); A. Esposito *et al.*, Phys. Rev. D **88**, no. 5, 054029 (2013).
- [22] T. W. Chiu *et al.* [TWQCD Collaboration], Phys. Rev. D **73**, 094510 (2006); C. Alexandrou *et al.*, JHEP **1304**, 137 (2013); M. Wagner *et al.*, J. Phys. Conf. Ser. **503**, 012031 (2014); S. Prelovsek *et al.*, Phys. Rev. D **91**, no. 1, 014504 (2015).
- [23] T. W. Chiu *et al.* [TWQCD Collaboration], Phys. Lett. B **646**, 95 (2007) [hep-ph/0603207].
- [24] C. B. Lang *et al.*, JHEP **1404**, 162 (2014); Phys. Rev. D **86**, 054508 (2012).
- [25] D. Mohler, S. Prelovsek and R. M. Woloshyn, Phys. Rev. D **87**, no. 3, 034501 (2013) [arXiv:1208.4059 [hep-lat]].
- [26] C. B. Lang *et al.*, Phys. Rev. D **84**, no. 5, 054503 (2011) [Erratum-ibid. D **89**, no. 5, 059903 (2014)] [arXiv:1105.5636 [hep-lat]].
- [27] K. Polejaeva and A. Rusetsky, Eur. Phys. J. A **48**, 67 (2012); R. A. Briceno and Z. Davoudi, Phys. Rev. D **87**, no. 9, 094507 (2013); M. T. Hansen and S. R. Sharpe, PoS LATTICE **2013**, 221 (2014); R. A. Briceno, arXiv:1311.6032 [hep-lat].
- [28] A. Hasenfratz, R. Hoffmann and S. Schaefer, Phys. Rev. D **78**, 054511 (2008); Phys. Rev. D **78**, 014515 (2008).
- [29] M. Peardon *et al.* [Hadron Spectrum Collaboration], Phys. Rev. D **80**, 054506 (2009) [arXiv:0905.2160 [hep-lat]].
- [30] C. Michael, Nucl. Phys. B **259**, 58 (1985); M. Lüscher, Commun. Math. Phys. **104**, 177 (1986); M. Lüscher and U. Wolff, Nucl. Phys. B **339**, 222 (1990); B. Blossier *et al.*, JHEP **0904**, 094 (2009);
- [31] M. Lüscher, Nucl. Phys. B **354**, 531 (1991), Commun. Math. Phys. **105**, 153 (1986); M. Döring *et al.*, Eur. Phys. J. A **47**, 139 (2011); M. T. Hansen and S. R. Sharpe, Phys. Rev. D **86**, 016007 (2012); R. A. Briceno, Phys. Rev. D **89**, no. 7, 074507 (2014);
- [32] J. J. Dudek *et al.* [Hadron Spectrum Collaboration], Phys. Rev. D **87**, no. 3, 034505 (2013) [Erratum-ibid. D **90**, no. 9, 099902 (2014)] [arXiv:1212.0830 [hep-ph]].
- [33] D. Mohler *et al.*, Phys. Rev. Lett. **111**, no. 22, 222001 (2013) [arXiv:1308.3175 [hep-lat]].
- [34] J. J. Dudek *et al.* [Hadron Spectrum Collaboration], Phys. Rev. Lett. **113**, no. 18, 182001 (2014) [arXiv:1406.4158 [hep-ph]].
- [35] S. Prelovsek *et al.*, Phys. Rev. D **88**, no. 5, 054508 (2013) [arXiv:1307.0736 [hep-lat]].
- [36] D. C. Moore and G. T. Fleming, Phys. Rev. D **74**, 054504 (2006).
- [37] C. Thomas, R. Edwards, J. Dudek, Phys. Rev. D **85**, 014507 (2012).
- [38] R. Briceno, Phys. Rev. D **89**, 074507 (2014).
- [39] R. Briceno, Z. Davoudi, T. Luu, Phys. Rev. D **88**, 034502 (2013).
- [40] R. Briceno, Z. Davoudi, T. Luu, M. Savage, Phys. Rev. D **88**, 114507 (2013).
- [41] A. X. El-Khadra, A. S. Kronfeld and P. B. Mackenzie, Phys. Rev. D **55**, 3933 (1997) [hep-lat/9604004].
- [42] C. B. Lang *et al.*, Phys. Rev. D **90**, no. 3, 034510 (2014) [arXiv:1403.8103 [hep-lat]].
- [43] A. Ali *et al.*, Phys. Rev. D **91**, no. 1, 017502 (2015) [arXiv:1412.2049 [hep-ph]].
- [44] J. F. Nieves and P. B. Pal, Am. J. Phys. **72**, 1100 (2004) [hep-ph/0306087].
- [45] S. Coleman. 1985. Aspects of Symmetry (Cambridge University Press, Cambridge, England.).
- [46] S. Weinberg, Phys. Rev. Lett. **110**, 261601 (2013); R. F. Lebed, Phys. Rev. D **88**, 057901 (2013); T. D. Cohen and R. F. Lebed, Phys. Rev. D **89**, no. 5, 054018 (2014).
- [47] L. Liu *et al.*, Hadron Spectrum Collaboration, JHEP **1207**, 126 (2012).
- [48] S. Sasaki and T. Yamazaki, Phys. Rev. D **74**, 114507 (2006).
- [49] I. V. Danilkin and Y. A. Simonov, Phys. Rev. Lett. **105**, 102002 (2010), Phys. Rev. D **81**, 074027 (2010); S. Coito, G. Rupp and E. van Beveren, Eur. Phys. J. C **71**, 1762 (2011), Eur. Phys. J. C **73**, no. 3, 2351 (2013); J. Ferretti, G. Galat and E. Santopinto, Phys. Rev. C **88**, no. 1, 015207 (2013)
- [50] M. Takizawa and S. Takeuchi, PTEP **2013**, 0903D01 (2013); S. Takeuchi, K. Shimizu and M. Takizawa, arXiv:1408.0973 [hep-ph].
- [51] D. Gamermann and E. Oset, Phys. Rev. D **80**, 014003 (2009) [arXiv:0905.0402 [hep-ph]].
- [52] N. A. Tornqvist, Phys. Lett. B **590**, 209 (2004) [hep-ph/0402237].
- [53] M. Jansen, H.-W. Hammer and Y. Jia, Phys. Rev. D **89**, no. 1, 014033 (2014); E. J. Garzon *et al.*, Phys. Rev. D **89**, no. 1, 014504 (2014); M. Albaladejo *et al.*, Phys. Rev. D **88**, no. 1, 014510 (2013).